

# MÁSTERES de la UAM

Facultad de Ciencias  
/ 15-16

Nanociencia



excelencia Campus Internacional UAM  
CSIC+



**Dendritic  
silicon-containing  
molecules:  
dendrimer-platinum(II)  
conjugates  
and its potential  
binding to quantum  
dots**

*Álvaro Doñoro Pina*



UNIVERSIDAD AUTÓNOMA DE MADRID

**DENDRITIC SILICON-CONTAINING MOLECULES:  
DENDRIMER-PLATINUM(II) CONJUGATES  
AND  
ITS POTENTIAL BINDING TO QUANTUM DOTS**

Master's Final Project

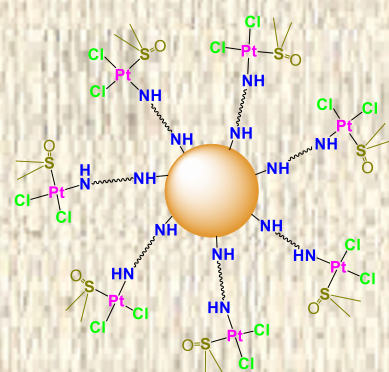
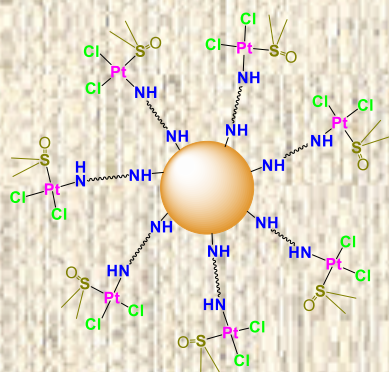
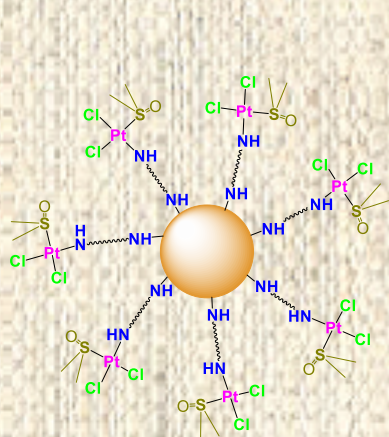
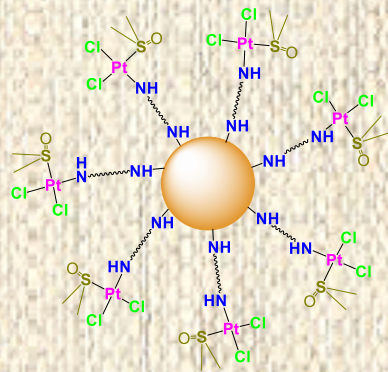
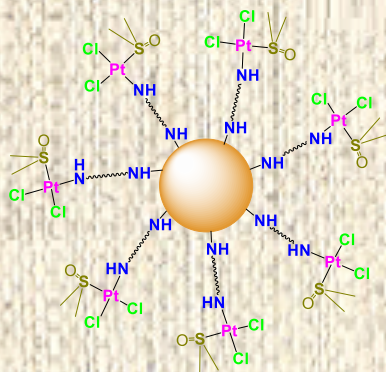
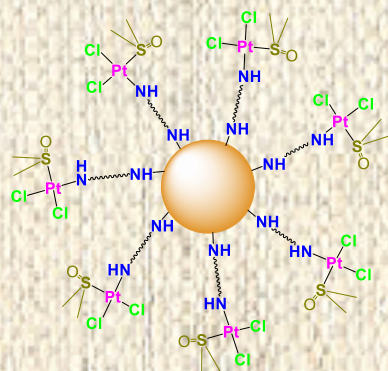
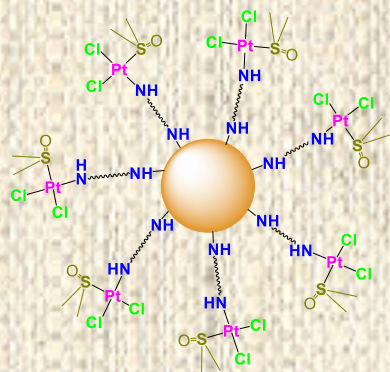
Álvaro Doñoro Pina

Inorganic Chemistry Department

September 2016

Directors: Dr. Ana M. González Vadillo

Dr. Isabel Cuadrado Sánchez



# Index

---

## Abstract

<b>1. Introduction</b>	<b>1</b>
<b>2. Objectives</b>	<b>5</b>
<b>3. Homo- and Heterobifunctionalized Organosiloxanes</b>	<b>6</b>
3.1. Synthesis of bifunctionalized siloxane precursors (1) and (2)	6
3.2. Synthesis of N-BOC protected siloxanes (3) and (4)	8
3.3. Synthesis of ferrocene-containing siloxane (5)	9
3.4. Characterization and structural studies of siloxanes (1) - (5)	9
3.4.1. Nuclear Magnetic Resonance: $^1\text{H}$ -NMR and $^{13}\text{C}$ -NMR	10
3.4.2. Infrared Spectroscopy	11
3.4.3. Mass Spectrometry	11
<b>4. Dendrimer-Platinum(II) Conjugates</b>	<b>12</b>
4.1. Synthesis of <i>cis</i> -[PtCl <sub>2</sub> (DMSO) <sub>2</sub> ] (6) complex	12
4.2. Synthesis of dendrimer-platinum(II) conjugate (7)	12
4.3. Characterization and structural study of siloxane (7)	13
4.3.1. Nuclear Magnetic Resonance: $^1\text{H}$ -NMR, $^{13}\text{C}$ -NMR and $^{195}\text{Pt}$ -NMR	13
4.3.2. Infrared Spectroscopy	14
4.3.3. Mass Spectrometry	15
<b>5. Surface Functionalization of Colloidal Nanocrystals</b>	<b>16</b>
5.1. Synthesis and characterization of colloidal nanocrystals	16
5.2. Study of the ligand exchange process	17
5.2.1. Ligand removal	17
5.2.2. Affinity study	17
5.2.3. Ligand exchange	19
<b>6. Experimental</b>	<b>21</b>
6.1. Synthesis of $\{(\text{CH}_3)_2\text{Si}[\text{p}-(\text{CH}_2)_2\text{C}_6\text{H}_4\text{NH}_2]\}_2\text{O}$ ((1)	21
6.2. Synthesis of N-BOC protected siloxanes (3) and (4) and ferrocene-containing siloxane (5)	22
6.3. Synthesis of <i>cis</i> -[PtCl <sub>2</sub> (DMSO) <sub>2</sub> ] (6) complex and dendrimer-platinum(II) conjugate (7)	23
6.4. General procedure for ligand exchange incubation	24
<b>7. Conclusions and Future Work</b>	<b>25</b>

# Abstract

---

Under the need to identify novel therapeutic strategies able to bring improved treatments, dendrimers present particular advantages, such as narrow polydispersity and multifunctional surface, offering versatility, both compositionally and structurally. From the pharmaceutical and biomedical point of view, these properties make them excellent candidates for evaluation as drug carriers, either by physical entrapment inside the dendritic structure or by covalent attachment onto surface or other functionalities to afford dendrimer-drug conjugates.

Regarding tumoral diseases, platinum complexes represent the first-line drugs used in therapy. They have good aqueous solubility but require drug delivery methods to reduce toxicity, side effects or enable targeting. Much research has been focused on these methods and one extensive area of them is concerned with improving the delivery of platinum anticancer drugs by polymer drug delivery, which may lead to reduced side effects and greater efficacy at lower doses of drug.

Additionally, a number of simple neutral ferrocene derivatives have been investigated in recent years as a novel class of medicinal compounds who exhibit cytotoxic behaviour and inhibit the development of tumors *in vivo*. In addition, the ferrocene unit has also been linked to platinum, palladium or ruthenium centres in order to achieve synergistic biological effects between the two active metals.

Furthermore, semiconductor nanoparticles, also called colloidal quantum dots, have proved to be suitable for biological applications, due to their tunable optical properties, their high optical stability and their carrier mobilities. In fact, the new generations of quantum dots have far-reaching potential for the study of intracellular processes at the single-molecule level, high-resolution cellular imaging, long-term *in vivo* observation of cell trafficking, tumor targeting, and diagnostics.

So, regarding all this background, this work tries to connect all these novel areas of research with nanobiology purposes, the synthesis of potentially cytotoxic dendrimer-platinum(II) conjugates whose properties and functionalities might be improved by its binding to different colloidal fluorescence nanocrystals.

# 1. Introduction

*Cis*-diamminedichlorideplatinum(II), or cisplatin ( $c\text{-[PtCl}_2(\text{NH}_3)_2]$ ), is one of the most effective anticancer agents that nowadays exists, but its clinical use is limited by a large amount of toxic side effects and platinum resistance processes. To avoid these problems, variations on the structure of this complex can be made in order to design new anticancer drugs (Figure 1). Non-leaving ligands (L-type) are generally nitrogen donors which form thermodynamically stable bonds with platinum. Consequently, they are preserved in the final Pt-DNA adduct and any modification in these ligands could directly affect its nature. On the other hand, leaving ligands

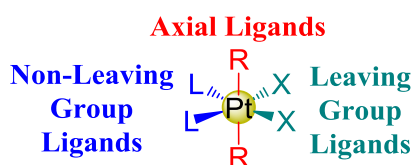


Figure 1.- Different ligands in platinum complexes

(X-type) are labile and they are lost before DNA binding. They mainly affect the reaction stoichiometry, solubility and aquation kinetics. Finally, axial ligands (R-type) are only present on platinum (IV) complexes and they can be used as points for linking tumor-target moieties or even nanoparticles.<sup>[1]</sup>

Nevertheless, besides all these possible modifications of the structure, and with the aim of improving the cytotoxic activity of *cis*- complexes, there have also been reported several platinum(II) complexes with different structural requirements (*trans*- complexes or polinuclear compounds), which also show antiproliferative properties.<sup>[2]</sup> In fact, multiple strategies try to improve in the biological activity, like, for instance, the introduction of other metallic moieties to generate a synergistic effect. Due to its remarkable properties (electrochemical reversibility, easy functionalization, high stability in aqueous and aerobic media, etc.), ferrocene and its derivatives have found many applications, including medicinal chemistry. Actually, numerous ferrocene derivatives have proven to be highly active, *in vitro* and *in vivo*, against several diseases (malaria, HIV, cancer, etc.).<sup>[3]</sup> That is the case of ferrocifen and hydroxiferrocifen (Figure 2), both based on the structure of tamoxifen, a chemotherapeutic agent widely used to treat hormone-dependent breast cancer<sup>[4]</sup> which displays important limitations and side effects.

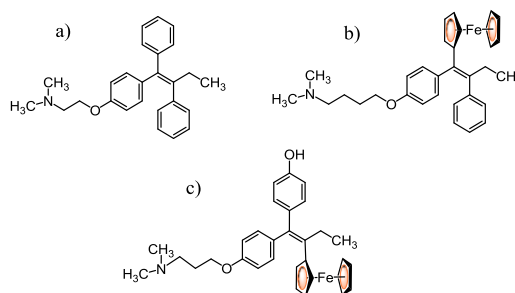


Figure 2.- Structures of a) Tamoxifen; b) Ferrocifen; c) Hydroxiferrocifen

<sup>1</sup> Wilson, J. J.; Lippard, S. J.; *Chem. Rev.* **2014**, *114*, 4470

<sup>2</sup> Messori, L.; Cubo, L.; Gabbiani, C.; Álvarez-Valdés, A.; Michelucci, E.; Pieraccini, G.; Rios-Luci, C.; León, L. G.; Padrón, J. M.; Navarro-Ranninger, C.; Casini, A.; Quiroga, A. G.; *Inorg. Chem.* **2012**, *11*, 1717

<sup>3</sup> Ornelas, C.; *New J. Chem.* **2011**, *35*, 1973

<sup>4</sup> Hartinger, C. G.; Metzler-Nolte, N.; Dyson, P. J.; *Organometallics*, **2012**, *31*, 5677

Although antitumor activity studies of heterometallic Pt(II)-ferrocene complexes are not too common, synergistic biological effects may arise from this type of compounds.<sup>[5]</sup> For this reason, our research group has had a longstanding interest in the preparation and study of ferrocenyl and platinum-based derivatives with antitumoral properties. Hence, the present work attempts to follow the guidelines of our previously published researches (Figure 3),<sup>[6]</sup> trying to reach solutions for some emerging problems, like the low solubility values that some of the complexes showed when they were tested in a biological medium.

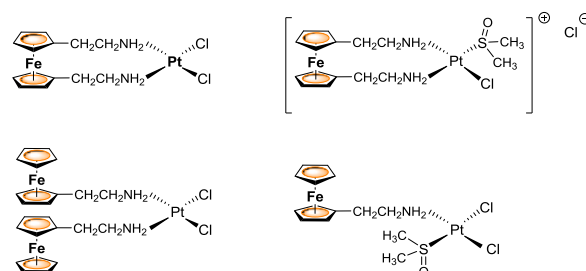


Figure 3.- Heterometallic complexes previously synthesized by our research group

With this purpose, we believe that the incorporation of silicon and, in consequence, the synthesis of organosilicon small molecules might be particularly interesting, considering that this strategy is an extensively used method to design, control and optimize stability, solubility and pharmacological properties. From a logical point of view, the sila-substitution (C/Si exchange) seems adequate because of the isosteric relationship between carbon and silicon, meaning that both elements have many similarities, but also differ substantially from one another (Table 1).<sup>[7]</sup>

Property	Carbon	Silicon
Covalent Radius	77 pm	117 pm
Bond Length	1.54 (for C-C bond)	1.87 (for Si-C bond)
Lipophilicity	Log <i>P</i> of PhCMe <sub>3</sub> : 4.0	Log <i>P</i> of PhSiMe <sub>3</sub> : 4.7
Electronegativity	2.50	1.74

Table 1.- Comparison of silicon and carbon properties relevant for medicinal chemistry

Some of these fundamental differences can lead to important alterations in the physicochemical and biological properties of silicon-containing analogues. As a matter of fact, these changes in the properties can contribute to enhance potency and pharmacological attributes.

In addition, the chemistry of silicon offers the possibility of carrying out a wide variety of chemical reactions. For instance, it is one of the most convenient elements used to prepare structural units in the synthesis of macromolecules, either linear polymers or dendrimers, due to the high stability of Si-C (carbosilanes), Si-O-C (carbosiloxanes) and Si-O-Si (siloxanes) bonds and its great reactivity towards many functional groups. Besides, carbosilanes and siloxanes are physiologically biocompatible. That is the reason why silicon-containing polymers and dendrimers could be suitable as drug carriers.

<sup>5</sup> Cortés, R.; Tarrado-Castellarnau, M.; Talancón, D.; López, C.; Link, W.; Ruiz, D.; Centelles, J. J.; Quitante, J.; Cascante, M.; *Metallomics*, **2014**, *6*, 622

<sup>6</sup> Nieto, D.; González-Vadillo, A. M.; Bruña, S.; Pastor, C. J.; Ríos-Luci, C.; León, L. G.; Padrón, J. M.; Navarro-Ranninger, C.; Cuadrado, I.; *Dalton Trans.* **2012**, *41*, 432

<sup>7</sup> Franz, A. K.; Wilson, S. O.; *J. Med. Chem.* **2013**, *56*, 388

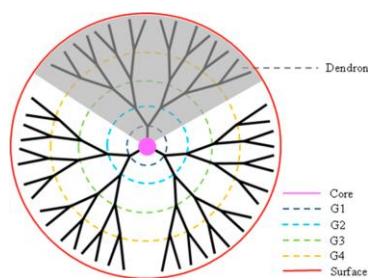


**Figure 4.-** Schematic illustration of dendrimer anatomy.

On its behalf, dendrimers are highly branched three-dimensional macromolecules with all bonds emanating from a central core, where dendrons are the repetitive units organized in layers (generations) surrounding the so mentioned core (Figure 4). These structures present particular advantages such as well-defined molecular structures (monodispersity), nanometer size range and a huge number of peripheral functionalities, offering polyvalence, both compositionally and structurally.<sup>[8]</sup>

Then, under the need to identify novel therapeutic strategies able to bring improved treatments, from the pharmaceutical and biomedical point of view, dendrimers versatility makes them excellent candidates for evaluation as biological agents, but they have to fulfil certain requirements.<sup>[9]</sup> The dendrimer should be:

- non-toxic
- able to cross biobarriers
- able to stay in circulation for the time needed to have a clinical effect
- able to target specific structures

Taking all these properties and demands into account, dendrimers can act as vehicles for solubilization, encapsulation or complexation (Figure 5), delivery and site-specific targeting of small-molecule drugs, biopharmaceuticals, and contrast agents.<sup>[10]</sup>

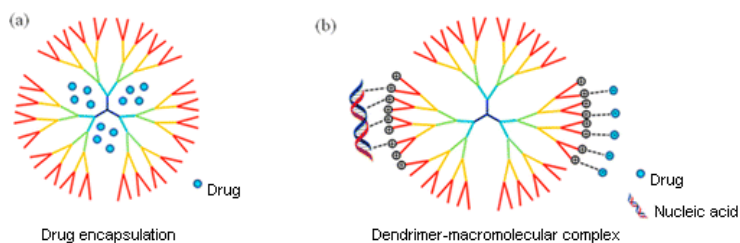


**Figure 5.-** Selected biomedical applications of dendrimers

In addition, new strategies have arisen from emerging fields like nanomedicine. Enhancing the selectivity for tumor tissue to mitigate toxic side effects and improve the clinical effectiveness and applicability is a critical goal. A wide variety of nanostructures might fulfil this purpose, from self-assembled nanoparticles<sup>[11]</sup> or encapsulating protein nanocages<sup>[12]</sup>, to magnetic nanoparticles<sup>[13]</sup> or colloidal nanocrystals.

<sup>8</sup> Hu Yang, H.; Kao, W. J.; *J. Biomater. Sci. Polymer Edn.* **2006**, *17*, 3

<sup>9</sup> Nanjwade, B. K.; Bechra, H. M. Derkar, G. K.; Manvi, F. V.; Nanjwade, V. K.; *Eur. J. Pharm. Sci.* **2009**, *38*, 185

<sup>10</sup> Wu, L.; Ficker, M.; Christensen, J. B.; Trohopoulos, P. N.; Moghimi, S. M.; *Bioconjugate Chem.* **2015**, *26*, 1198

<sup>11</sup> Cheng, Q.; Shi, H.; Huang, H.; Cao, Z.; Wang, J.; Liu, Y.; *Chem. Commun.* **2015**, *51*, 17536

<sup>12</sup> Pontillo, N.; Pane, F.; Messori, L.; Amoresano, A.; Merlino, A.; *Chem. Commun.* **2016**, *52*, 4136

<sup>13</sup> Medrikova, Z.; Novohradsky, V.; Zajac, J.; Vrána, O.; Kasparkova, J.; Bakandritsos, A.; Petr, M.; Zboril, R.; Brabec, V.; *Chem. Eur. J.* **2016**, *22*, 1

Colloidal nanocrystals (NCs) have become an important class of material with potential applications ranging from electronic devices to medicine.<sup>[14]</sup> NCs comprise an inorganic crystalline core (which can contain core-shell structures such as in the case of CdSe/ZnS) and, in the context of biological environments, an organic coating (either by design or by adsorption of proteins). Thus, even when the inorganic NC cores act only as passive carriers, the possibility to link different functional molecules to their organic surface coating enables multifunctionality (targeting, contrast for imaging, etc.). However, the NC cores may also introduce functionality, such as fluorescence or super-paramagnetism. Therefore, with inorganic cores and organic shells together, NCs are suitable for combining different functionalities to achieve remarkable and observable properties (like imaging through fluorescence microscopy or magnetic resonance imaging).

As fluorescent labelling in biology (for both *in vivo* and *in vitro* assay detection) has become fundamental to understand the interplay of biomolecules, and the photophysical properties of organic fluorophores (narrow absorption and broad emission spectra) limit their effectiveness in long-term imaging, quantum dots (QDs) have awakened interest because of their broad absorption spectra, allowing excitation by a wide range of wavelengths; narrow emission spectra, which can be modified to emit light from ultraviolet to infrared by variation of core size and composition and surface coatings; and good photostability, that enables long fluorescence lifetime.<sup>[15][16][17]</sup>

Most emissions of biological areas of interest fall in the visible - near infrared region. Near-infrared light (700 - 2500 nm) can penetrate biological tissues, such as skin and blood, more efficiently than visible light because of their less absorption and scattering at longer wavelengths, which diminishes at longer wavelengths than 950 nm owing to the absorption by water and lipids). Thus, a clear window exists between 650 - 950 nm for optical imaging of live animals but, in practice, this window is not optimal because tissue autofluorescence produces background noise and the tissue penetration depth is limited. That is why recent efforts have been devoted to identify agents that emit in the so called second near-infrared window (1000 – 1400 nm), due to minimal autofluorescence and low tissue scattering of this region (Figure 6).<sup>[18]</sup>

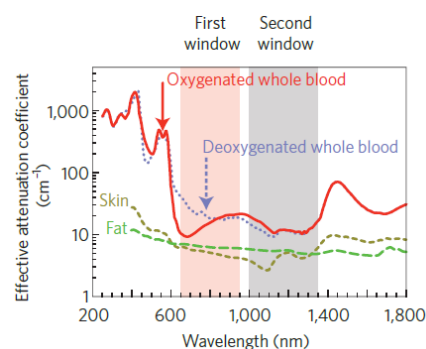


Figure 6.- Optical windows in biological tissues

<sup>14</sup> Kovalenko, M. V.; Manna, L.; Cabot, A.; Hens, Z.; Talapin, D. V.; Kagan, C. R.; Klimov, V. I.; Rogach, A. L.; Reiss, P.; Milliron, D. J.; Guyot-Sionnest, P.; Konstantatos, G.; Parak, W. J.; Hyeon, T.; Korgel, B. A.; Murray, C. B.; Heiss, W.; *ACS Nano*, **2015**, *9* (2), 1012

<sup>15</sup> Michalet, X.; Pinaud, F. F.; Bentolila, L. A.; Tsay, J. M.; Doose, S.; Li, J. J.; Sundaresan, G.; Wu, A. M.; Gambhir, S. S.; Weiss, S.; *Science*, **2005**, *307*, 538

<sup>16</sup> Medintz, I. L.; Uyeda, H. T.; Goldman, E. R.; Mattoussi, H.; *Nature Materials*, **2005**, *4*, 435

<sup>17</sup> Jamieson, T.; Bakhshi, R.; Petrova, D.; Pockock, R.; Imani, M.; Seifalian, A. M.; *Biomaterials*, **2007**, *28*, 4717

<sup>18</sup> Smith, A. M.; Mancini, M. C.; Nie, S.; *Nat. Nanotechnol.* **2009**, *4*, 710

## 2. Objectives

---

Regarding all this background, and since we are focused on the chemistry of ferrocenyl-containing compounds and dendrimers,<sup>[19]</sup> and on the preparation and study of platinum-based derivatives with antitumoral properties,<sup>[6]</sup> we became interested in using poly(dimethylsiloxy)silanes as useful precursors of silicon-containing ferrocenyl compound polymers, due to the high reactivity that Si-H bonds show against vinyl-functionalized compounds through hydrosilylation reactions. With this goal in mind, the initial work plan consisted in:

- ✿ Synthesizing, purifying and characterizing a new family of amino-functionalized silicon-containing dendrimers.
- ✿ Synthesizing, purifying and characterizing novel heterogeneous dendritic molecules containing ferrocene and amine units.
- ✿ Preparing and characterizing new heterometallic compounds based on ferrocene, silicon and platinum.

At the same time, we believed that these compounds may have the possibility of being linked to quantum dots, which could strongly increase their properties, not only chemically but also physically, because of the remarkable optical properties of this kind of nanoparticles. Therefore, we extended our work plan in order to carry out:

- ✿ Ligand exchange studies between several precursors and a wide variety of quantum dots to fully understand and optimize the ligand exchange process.
- ✿ Ligand exchange incubations between the heterometallic synthesized compounds and those quantum dots that showed better results in the model studies.

---

<sup>19</sup> Cuadrado, I. In *Silicon-Containing Dendritic Polymers*; Dvornic, P., Owen, M. J., Springer, 2009; 141

## 3. Homo- and Heterofunctionalized Organosiloxanes

### 3.1. Synthesis of bifunctionalized siloxane precursors (1) and (2)

The catalytic addition of silicon hydrides to carbon-carbon multiple bonds has proven to be an efficient method for the formation of organosilicon compounds and it is a widely applied process in the synthesis of functionalized organosilanes and for the production of silicon polymers. Nowadays, the most versatile catalyst is Karstedt's (Figure 7), a platinum(0) complex containing vinyl-siloxane ligands that shows higher catalytic activity than other platinum catalyst like Speier's ( $\text{H}_2[\text{PtCl}_6]$ ).<sup>[20]</sup>

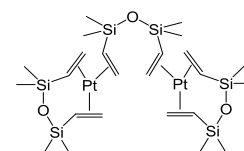
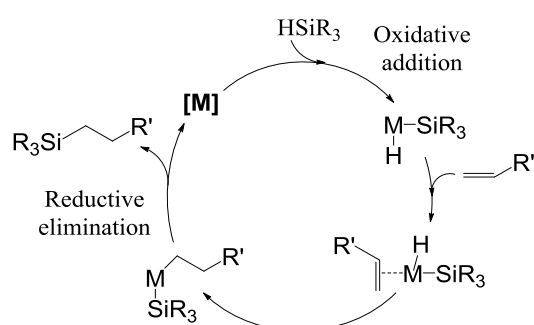


Figure 7.- Structure of Karstedt's catalyst



Scheme 1.- Chalk-Harrod's mechanism for the coordination-catalyzed hydrosilylation of olefins.

The hydrosilylation of olefins catalyzed by platinum complexes can be explained through Chalk-Harrod's mechanism (Scheme 1). The first step of this mechanism establishes an oxidative addition of the silane to the catalyst for the Si-H bond activation; secondly, the olefin undergoes alkene insertion to the M-H bond; finally, the reductive elimination leads to the formation of the Si-C bond.<sup>[21]</sup>

Consequently, due to the high reactivity that Si-H bonds show against vinyl-functionalized compounds, we became interested in using poly(dimethylsiloxy)silanes as useful precursors of silicon-containing amino-functionalized dendritic molecules that could not only coordinate to one or two platinum(II) moieties but also have other functionalities, such as ferrocene, looking for the so called synergistic effect between the two metal units. With this premise, we selected two small but highly branched siloxanes which would serve as suitable starting materials (Figure 8).

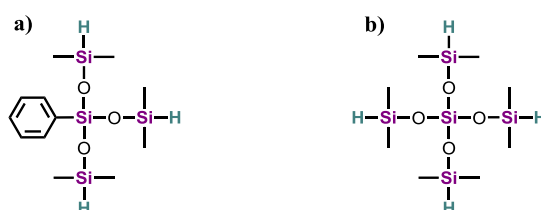


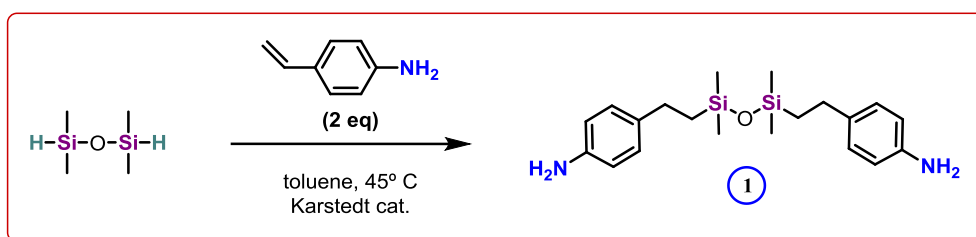
Figure 8.- Structures of: a) Tris(dimethylsiloxy)phenylsilane; b) Tetrakis(dimethylsiloxy)silane

<sup>20</sup> Troegel, D.; Stohrer, J.; *Coord. Chem. Rev.* **2011**, 255, 1440

<sup>21</sup> Chalk, A. J.; Harrod, J. F.; *J. Am. Chem. Soc.* **1965**, 87, 16

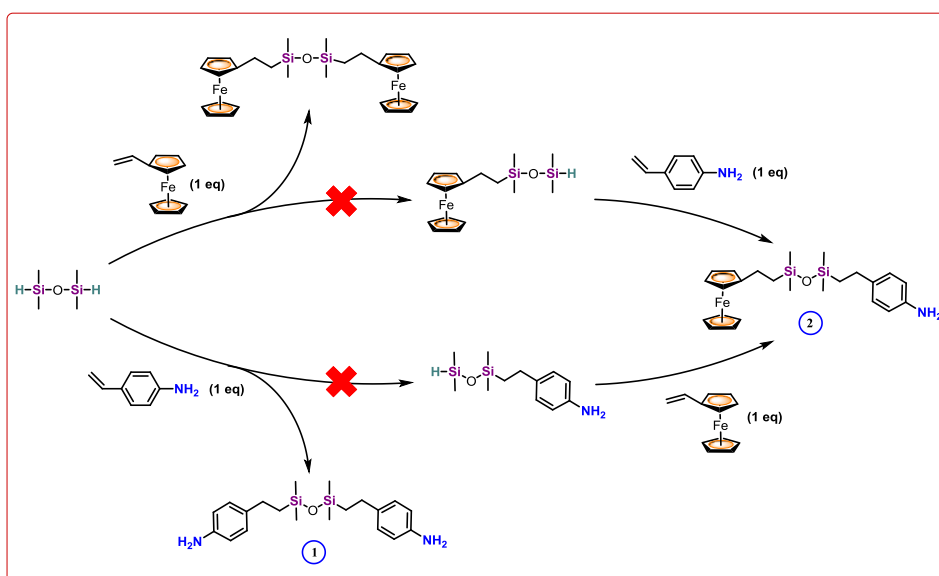
Nevertheless, when developing new chemical systems, it is of vital importance to gain a deep understanding of chemical reaction processes. For this reason, we decided to start with a simpler silane structure, a linear one, to carry out model reactions.

Thus, hydrosilylation reaction between one equivalent of 1,1,3,3-tetramethyldisiloxane and two equivalents of 4-vinylaniline, at 45° C, using toluene as solvent (Scheme 2), led to the formation of  $\{(\text{CH}_3)_2\text{Si}[p\text{-(CH}_2)_2\text{C}_6\text{H}_4\text{NH}_2]\}_2\text{O}$  (**1**), which was obtained as a yellow oil.



Scheme 2.- Synthesis of  $\{(\text{CH}_3)_2\text{Si}[p\text{-(CH}_2)_2\text{C}_6\text{H}_4\text{NH}_2]\}_2\text{O}$  (**1**)

On the other hand, the synthesis of bifunctionalized ferrocene-amino siloxane  $\{[p\text{-NH}_2\text{C}_6\text{H}_4(\text{CH}_2)_2]\text{Si}(\text{CH}_3)_2\text{O}\{(\text{CH}_3)_2\text{Si}[(\text{CH}_2)_2(\text{Fc})]\}$  (**2**) (Fc =  $(\eta^5\text{-C}_5\text{H}_4)\text{Fe}(\eta^5\text{-C}_5\text{H}_5)$ ) was attempted by selective hydrosilylation in two steps (Scheme 3). However, the one-equivalent addition of vinylferrocene to one equivalent of 1,1,3,3-tetramethyldisiloxane always led to the formation of the homofunctionalized siloxane, probably due to the high reactivity of this vinylic reagent against hydrosilylation. Consequently, looking for better results, the order of the reagents was modified. In this case, although (**1**) appeared as the majoritary product, the Si-H bond of the monosubstituted siloxane could be identified by  $^1\text{H-NMR}$ . Unfortunately, purification resulted unsuccessful because of the high interaction between Si-H bonds with silica and alumina, ending up in the total retention of the product in the chromatography column.



Scheme 3.- Synthesis of  $\{(\text{CH}_3)_2\text{Si}[p\text{-(CH}_2)_2\text{C}_6\text{H}_4\text{NH}_2]\}_2\text{O}\{(\text{CH}_3)_2\text{Si}[(\text{CH}_2)_2(\text{Fc})]\}$  (**2**)

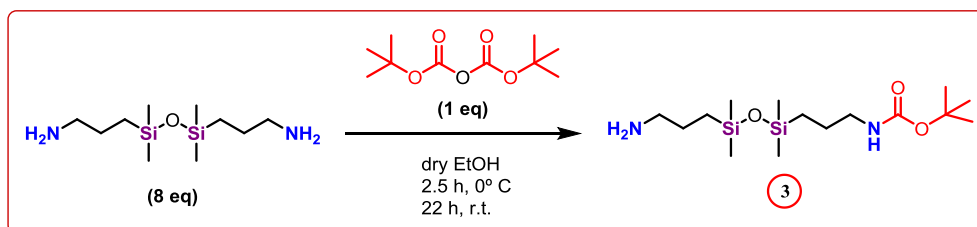
### 3.2. Synthesis of N-BOC protected siloxanes (3) and (4).

Monofunctionalization of symmetrical or unsymmetrical diamines is an essential step for the synthesis of biologically important pharmacores and materials. Among the various amine protecting groups, BOC (*tert*-butyloxycarbonyl) is the most popular, and its protected form is normally in a good physical state to be handled for the next reaction.

Under the strong possibility of (1) leading to undesired multimetallic structures when reacting with platinum(II) complexes due to the identically-reactive amine positions, selective amine monoprotection resulted essential. In addition, selective BOC protection offers the possibility of adding different substituents to equally-reactive positions and, in our case, it ended up being an essential key for further ferrocene functionalization.

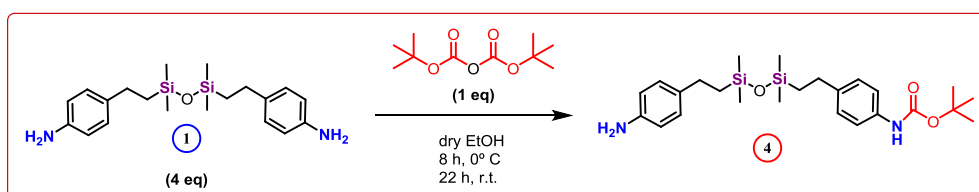
Although some publications suggested room temperature or even heating reaction conditions,<sup>[22][23]</sup> very poor yields were obtained through these methods. However, by modifying some literature procedures,<sup>[24][25]</sup> a very slow addition of (BOC)<sub>2</sub>O (di-*tert*-butyl dicarbonate) at 0° C, with a tight control of the concentration, turned out to be the ideal reaction conditions.

In this way, {BOCNH(CH<sub>2</sub>)<sub>3</sub>Si(CH<sub>3</sub>)<sub>2</sub>}O{(CH<sub>3</sub>)<sub>2</sub>Si(CH<sub>2</sub>)<sub>3</sub>NH<sub>2</sub>} (3) was obtained by reacting an excess of commercially available 1,3-bis(3-aminopropyl)-1,1,3,3-tetramethyldisiloxane with one equivalent of (BOC)<sub>2</sub>O in dry ethanol (Scheme 4).



Scheme 4.- Synthesis of {BOCNH(CH<sub>2</sub>)<sub>3</sub>Si(CH<sub>3</sub>)<sub>2</sub>}O{(CH<sub>3</sub>)<sub>2</sub>Si(CH<sub>2</sub>)<sub>3</sub>NH<sub>2</sub>} (3)

Synthesis of {BOCNH[*p*-C<sub>6</sub>H<sub>4</sub>(CH<sub>2</sub>)<sub>2</sub>]Si(CH<sub>3</sub>)<sub>2</sub>}O{(CH<sub>3</sub>)<sub>2</sub>Si[*p*-(CH<sub>2</sub>)<sub>2</sub>C<sub>6</sub>H<sub>4</sub>NH<sub>2</sub>]} (4) (Scheme 5) was carried out with new modifications in respect of the previously described method. The diamine excess was largely reduced and (BOC)<sub>2</sub>O addition period was increased from 2.5 h to 8 h.



Scheme 5.- Synthesis of {BOCNH[*p*-C<sub>6</sub>H<sub>4</sub>(CH<sub>2</sub>)<sub>2</sub>]Si(CH<sub>3</sub>)<sub>2</sub>}O{(CH<sub>3</sub>)<sub>2</sub>Si[*p*-(CH<sub>2</sub>)<sub>2</sub>C<sub>6</sub>H<sub>4</sub>NH<sub>2</sub>]} (4)

<sup>22</sup> Lee, D. W.; Ha, H. J.; Lee, W. K.; *Synth. Commun.* **2007**, *37*, 737

<sup>23</sup> Van Houtem, M. C. H. J.; Martín-Rapún, R.; Vekemans, J. A. J. M.; Meijer E. W.; *Chem. Eur. J.* **2010**, *16*, 2258

<sup>24</sup> Krapcho, A. P.; Kuel, C. S.; *Synth. Commun.* **1990**, *20*, 2559

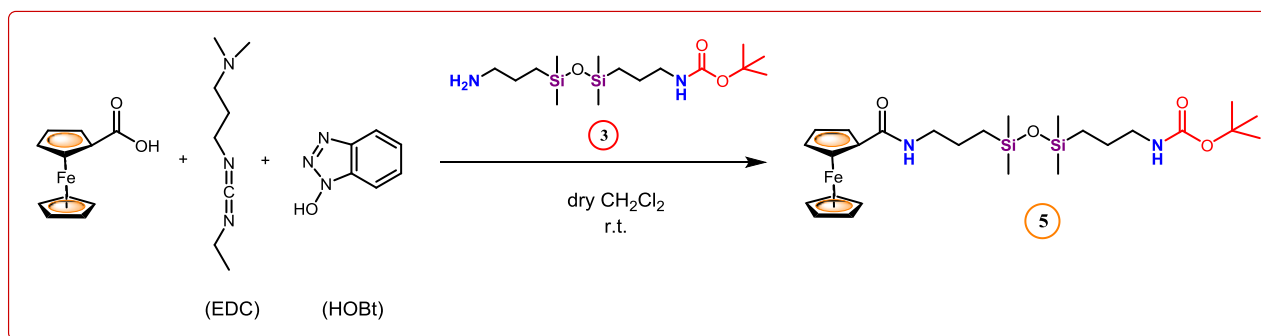
<sup>25</sup> Chan, P. C. M.; Roon, R. J.; Koerner, J. F.; Taylor, N. J.; Honek, J. F.; *J. Med. Chem.* **1995**, *38*, 4433

### 3.3. Synthesis of ferrocene-containing siloxane (5)

Since the hydrosilylation reaction with vinylferrocene proved to be unfruitful, ferrocene-amide formation appeared as a very adequate alternative to introduce the ferrocene unit. The formation of amide bonds by condensation of amines with carboxylic acids in the presence of carbodiimides is one of the most common synthetic procedures. To optimize these couplings, additives such as *N*-hydroxybenzotriazole (HOBt) are widely used as catalyst for the generation of active esters, capable of efficient acylation of amino groups.<sup>[26]</sup>

Therefore, {BOCNH(CH<sub>2</sub>)<sub>3</sub>Si(CH<sub>3</sub>)<sub>2</sub>}O{(CH<sub>3</sub>)<sub>2</sub>Si(CH<sub>2</sub>)<sub>3</sub>NHCOFc} (5) was synthesized by reacting ferrocene carboxylic acid and *N*-(3-Dimethylaminopropyl)-*N'*-ethylcarbodiimide (EDC) to produce the EDC-derived urea, which reacted with HOBt to give the HOBt ester. Finally, the addition at room temperature of N-BOC monoprotected diamine (3) led to the formation of the corresponding amide (Scheme 6).<sup>[27]</sup>

It must be noticed that modifications from the literature were made in order to improve the final yield. Ferrocene carboxylic acid, EDC and HOBt were added under argon atmosphere, at 0° C and using dry dichloromethane (CH<sub>2</sub>Cl<sub>2</sub>) as solvent.<sup>[28]</sup>



Scheme 6.- Synthesis of {BOCNH(CH<sub>2</sub>)<sub>3</sub>Si(CH<sub>3</sub>)<sub>2</sub>}O{(CH<sub>3</sub>)<sub>2</sub>Si(CH<sub>2</sub>)<sub>3</sub>NHCOFc} (5)

### 3.4. Characterization and structural studies of organosiloxanes (1) – (5)

As none of the synthesized compounds had been previously reported, a detailed characterization was accomplished by multinuclear Nuclear Magnetic Resonance Spectroscopy (NMR), Fourier Transform Infrared Spectroscopy (FT-IR) and Mass Spectrometry (MS).

<sup>26</sup> Chan, L. C.; Cox, B. G.; *J. Org. Chem.* **2007**, *72*, 8863

<sup>27</sup> Zhou, H. Y.; Li, M.; Qu, J.; Jing, S.; Xu, H.; Zhao, J. Z.; Zhang, J.; He, M. F.; *Organometallics*, **2016**, *35*, 1866

<sup>28</sup> Singh, M.; Argade, N. P.; *Synthesis*, **2012**, *44*, 3797

### 3.4.1. Nuclear Magnetic Resonance (NMR): $^1\text{H}$ -NMR and $^{13}\text{C}$ -NMR

Many similarities were found when analysing the NMR spectra of (1) - (5) because of the structural shared pattern (Figure 9). For instance, both Si-CH<sub>3</sub> and Si-CH<sub>2</sub> protons appeared at very similar shifts in all the compounds.

Nevertheless, a thorough characterization was needed for the AA'BB' aromatic systems of (1) and (4) and for the four different -CH<sub>2</sub>- groups of (3). So, for a proper assignment, Heteronuclear Multiple-Quantum Correlation Spectroscopy (HMQC), which detects correlation between two different nuclei that are separated by one bond, was required.

Regarding N-BOC protected compounds (1), (3) and (4), -NH<sub>2</sub> protons were easily identified when D<sub>2</sub>O was added to the NMR sample. Moreover, as it was expected, the deshielding ester moiety shifted downfield the corresponding -NH- signals.

Besides, the  $^1\text{H}$ -NMR spectra of (5) showed the typical pattern for monosubstituted ferrocene derivatives, a singlet for the C<sub>5</sub>H<sub>5</sub> moiety and two pseudo-triplets (which appeared as broad singlets) for the C<sub>5</sub>H<sub>4</sub> moiety.

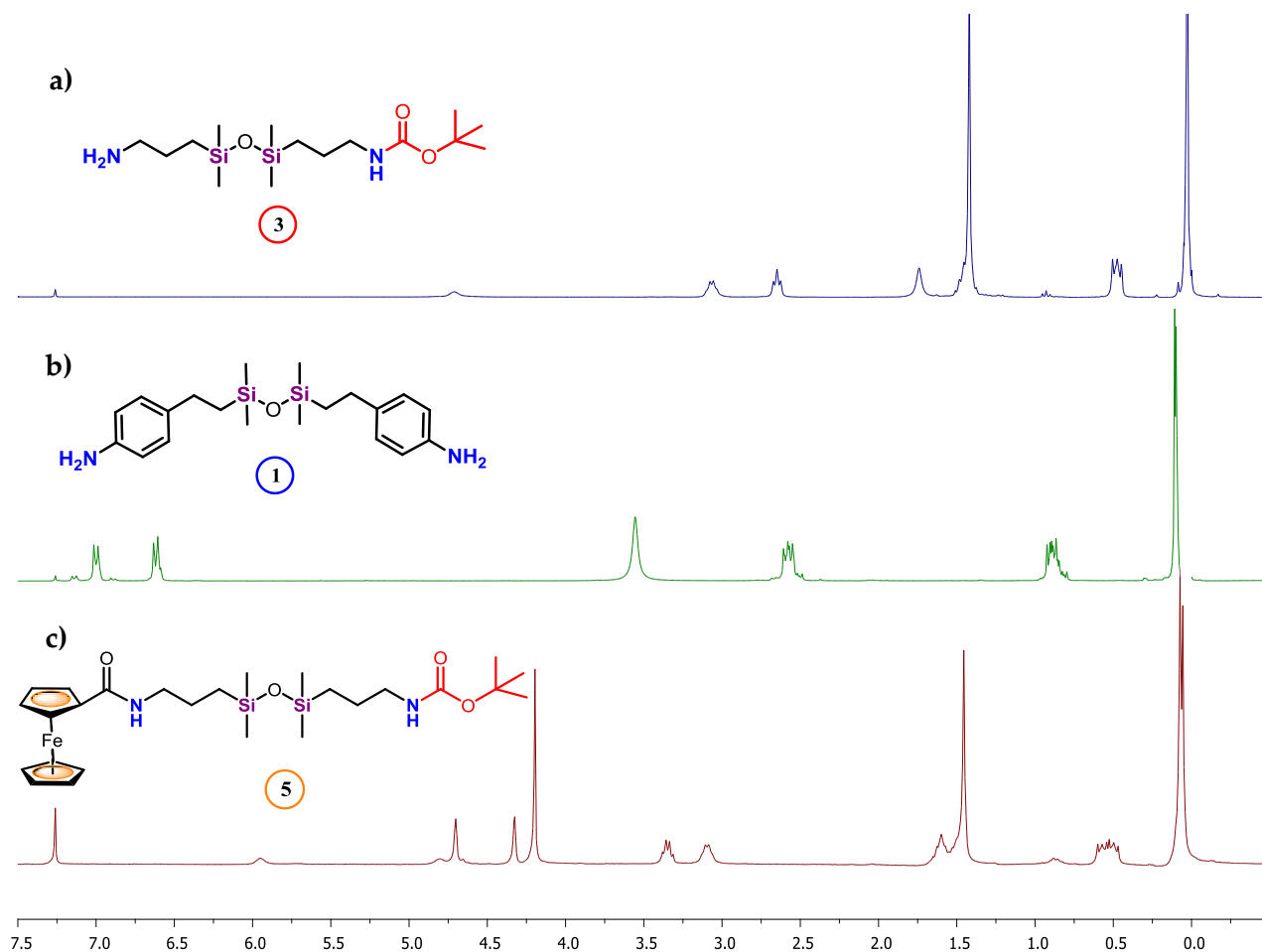


Figure 9.-  $^1\text{H}$  NMR spectra of a)  $\{(\text{CH}_3)_2\text{Si}(\text{CH}_2)_3\text{NHBOC}\}_2\text{O}$  ( $\text{CH}_3)_2\text{Si}(\text{CH}_2)_3\text{NH}_2$  (3), b)  $\{(\text{CH}_3)_2\text{Si}[\text{p}-(\text{CH}_2)_2\text{C}_6\text{H}_4\text{NH}_2]\}_2\text{O}$  (1) and c)  $\{(\text{CH}_3)_2\text{Si}(\text{CH}_2)_3\text{NHBOC}\}_2\text{O}$   $\{(\text{CH}_3)_2\text{Si}(\text{CH}_2)_3\text{NHCOFc}\}$  (5)

### 3.4.1. Infrared Spectroscopy (FT-IR)

Common features were found in the infrared spectra of **(1)** – **(5)**. The Si-O-Si typical stretching vibration appeared as a strong band in the region of 1000 – 1130  $\text{cm}^{-1}$ . In addition, a strong and sharp band at about 1260  $\text{cm}^{-1}$  corresponded to Si-CH<sub>3</sub> stretching vibration, together with one strong band in the range of 750 – 865  $\text{cm}^{-1}$ .<sup>[29]</sup>

Although Fermi doublet (3300 – 3500  $\text{cm}^{-1}$ ) could be identified as -NH<sub>2</sub> stretching vibrations, together with strong bands at 1550 – 1650  $\text{cm}^{-1}$  corresponding to -NH<sub>2</sub> scissoring vibration, **(3)** and **(4)** presented broad bands in the region of 3300 – 3700  $\text{cm}^{-1}$ , which could be due to the -NH- stretching vibration.

As it was expected, aromatic carbon-carbon stretching vibration bands were found in the range of 1500 – 1600  $\text{cm}^{-1}$  for **(1)** and **(4)**, as well as C=O stretching bands at about 1700  $\text{cm}^{-1}$  for **(3)**, **(4)** and **(5)**. In addition, **(5)** presented a strong and sharp Fe-Cp stretching vibration band at 484  $\text{cm}^{-1}$ , together with another strong and sharp band at 503  $\text{cm}^{-1}$  corresponding to the Cp tilt.

### 3.4.1. Mass Spectrometry (MS)

A very high fragmentation was observed when analysing **(1)** – **(5)** Mass Spectrometry spectra. For this reason, soft ionization techniques were required.

Since they are relatively low fragmentation techniques which mostly produce protonated ([M+H]<sup>+</sup>) or deprotonated ([M-H]<sup>-</sup>) molecules, Fast Atom Bombardment (FAB), Electrospray Ionization (ESI) or Matrix-Assisted Laser Desorption/Ionization (MALDI) turned to be the most adequate techniques to perform these analysis.

The most relevant detected ions for each compound are shown in Table 2. It must be noticed that all compounds were in total agreement with their calculated and experimental isotopic distributions.

Compound	Assignment	m/z (Da)	Ionization Technique
<b>(1)</b>	[M] <sup>+</sup>	372.0	FAB
	[M+H] <sup>+</sup>	373.0	
<b>(3)</b>	[M+H] <sup>+</sup>	349.3	MALDI
<b>(4)</b>	[M+H] <sup>+</sup>	473.3	ESI
<b>(5)</b>	[M+H] <sup>+</sup>	561.3	

Table 2.- Mass Spectrometry data for compounds **(1)** to **(5)**

<sup>29</sup> Launer, P. J.; *Silicone Compounds Register and Review*; Petrarch Systems, 1987, 100

## 4. Dendrimer-Platinum(II) Conjugates

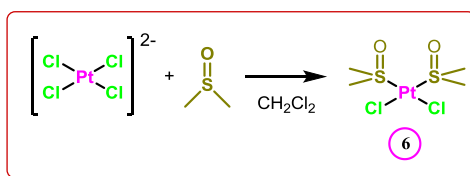
As we mentioned before, one of our main objectives was the synthesis of platinum(II)-based compounds with potential antitumoral properties.

The use of  $K_2[PtCl_4]$  (potassium tetrachlorideplatinate(II)) salt as a platinum(II) source requires a two-phased system due to the insolubility of this salt and the ligands in organic solvents and water, respectively. For this reason, reactions with  $K_2[PtCl_4]$  need a solvent mixture (generally, ethanol/water) and vigorous stirring so that the reaction can take place in the interface through phase-transfer between solvent layers.

In contrast, the use of *cis*- $[PtCl_2(DMSO)_2]$  (*cis*-dichloridebis(dimethylsulfoxide)platinum(II)) complex allows one-phase reactions because the organic ligand and the platinum(II) complex are both soluble in the same organic solvent.

### 4.1. Synthesis of *cis*- $[PtCl_2(DMSO)_2]$ (6) complex

Platinum(II) complex *cis*- $[PtCl_2(DMSO)_2]$  (6) was obtained by reaction at room temperature between DMSO (dimethylsulfoxide) and  $K_2[PtCl_4]$  as a crystalline yellow solid in which the DMSO coordinates to the metal centre through the sulphur atom (Scheme 7).<sup>[30]</sup>



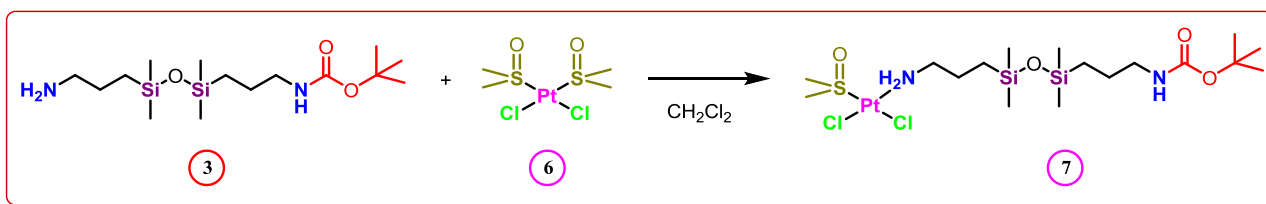
Scheme 7.- Synthesis of *cis*- $[PtCl_2(DMSO)_2]$  (6) complex

### 4.2. Synthesis of dendrimer-platinum(II) conjugate *cis*- $[PtCl_2(DMSO)_2]\{[NH_2(CH_2)_3O]Si\{O(CH_2)_3NHBOC\}\}$ (7)

As outlined above, the low solubility of  $K_2[PtCl_4]$  in organic solvents requires the use of water as reaction cosolvent. For this reason, we considered interesting the use of *cis*- $[PtCl_2(DMSO)_2]$  (6) complex, which is soluble in organic solvents, as a promising alternative to  $K_2[PtCl_4]$  when preparing new platinum complexes.

Therefore, *cis*- $[PtCl_2(DMSO)_2]\{[NH_2(CH_2)_3O]Si(CH_3)_2O\{[CH_3]_2Si(CH_2)_3NHBOC\}\}$  (7) was obtained by one-phase reaction between  $\{BOCNH(CH_2)_3Si(CH_3)_2O\{[CH_3]_2Si(CH_2)_3NH_2\}$  (3) and *cis*- $[PtCl_2(DMSO)_2]$  (6) in  $CH_2Cl_2$ , resulting in a yellow oil (Scheme 8).

<sup>30</sup> Price, J. H.; Williamson, A. N.; Schramm, R. F.; Wayland, B. B; *Inorg. Chem.* **1972**, *11*, 1280



Scheme 8.- Synthesis of *cis*-[PtCl<sub>2</sub>(DMSO)]((NH<sub>2</sub>(CH<sub>2</sub>)<sub>3</sub>Si(CH<sub>3</sub>)<sub>2</sub>)O((CH<sub>3</sub>)<sub>2</sub>Si(CH<sub>2</sub>)<sub>3</sub>NHBOC))]

As it was observed after a detailed characterization, coordination of (3) to the platinum centre resulted in a *cis*- geometry where just one DMSO ligand was displaced, leading to a NCl<sub>2</sub>S coordination environment.

### 4.3. Characterization and structural study of dendrimer-platinum(II) conjugate (7)

The structural identity of the novel molecule (7) was straight-forwardly established by Multinuclear NMR, FTIR and MS.

#### 4.3.1. Nuclear Magnetic Resonance (NMR): <sup>1</sup>H-NMR, <sup>13</sup>C-NMR and <sup>195</sup>Pt-NMR

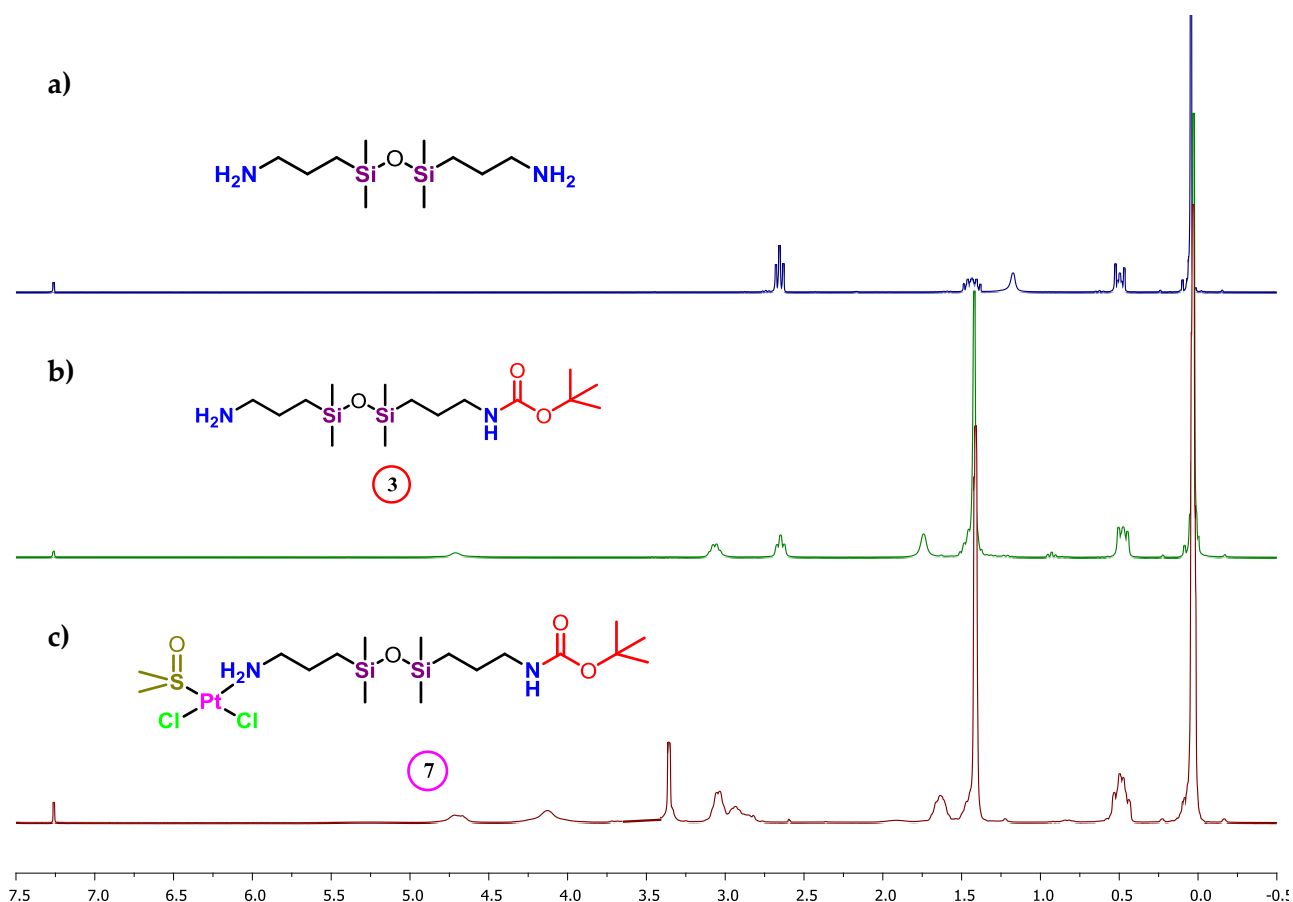


Figure 10.- <sup>1</sup>H NMR spectra of a) 1,3-bis(3-aminopropyl)-1,1,3,3-tetramethyl-1,3-dioxane, b) [BOCNH(CH<sub>2</sub>)<sub>3</sub>Si(CH<sub>3</sub>)<sub>2</sub>]O((CH<sub>3</sub>)<sub>2</sub>Si(CH<sub>2</sub>)<sub>3</sub>NH<sub>2</sub>) (3) and c) *cis*-[PtCl<sub>2</sub>(DMSO)]((NH<sub>2</sub>(CH<sub>2</sub>)<sub>3</sub>Si(CH<sub>3</sub>)<sub>2</sub>)O((CH<sub>2</sub>)<sub>3</sub>Si(CH<sub>3</sub>)<sub>2</sub>NHBOC))]

As it was expected,  $^{13}\text{C}$ -NMR and  $^1\text{H}$ -NMR spectrum of **(7)** were very similar to **(1)** (Figure 10), although a remarkable feature could be observed. The chemical shift of the  $-\text{NH}_2$  group of the ligand was considerably shifted downfield (4.14 ppm) in comparison with the corresponding free ligand signal (1.43 ppm). In addition, it was also possible to observe an intense singlet at 3.38 ppm, corresponding to the protons of the DMSO coordinated ligand, which clearly differ from the ones of the free DMSO ligand ( $\sim 2.50$  ppm).

The  $^{195}\text{Pt}$ -NMR resonance is extremely sensitive to the coordination environment, so the  $^{195}\text{Pt}$ -NMR spectrum of **(7)** provided convincing evidence for its coordination sphere and structure. A signal at -3068 ppm was detected, which was consistent with a  $\text{NCl}_2\text{S}$  set of donor atoms around the platinum centre.<sup>[31]</sup>

#### 4.3.2. Infrared Spectroscopy (FTIR)

Apart from the mentioned vibration bands of **(3)**, the IR spectrum of **(7)** showed two bands at  $324\text{ cm}^{-1}$  and  $342\text{ cm}^{-1}$ , due to the stretching of the Pt-Cl, according to a *cis*- structure.<sup>[32]</sup> Besides, stretching bands were found for S=O and Pt-S at  $1123\text{ cm}^{-1}$  and  $444\text{ cm}^{-1}$  respectively.<sup>[30]</sup>

#### 4.3.3. Mass Spectrometry (MS)

As very high fragmentation was observed again, a soft ionization technique was required. In this case, Electrospray Ionization (ESI) confirmed the proposed structure, with an excellent agreement between calculated and experimental isotopic distribution. Table 3 informs about the most relevant detected ions.

Compound	Assignment	m/z (Da)	Ionization Technique
(7)	$[\text{M}-\text{Cl}]^+$	657	ESI
	$[\text{M}+\text{H}]^+$	693	

Table 3.- Mass Spectrometry data of **(7)**

<sup>31</sup> Nedelec, N.; Rochon, F. D.; *Inorg. Chim. Acta*, **2001**, 319, 95

<sup>32</sup> Pantoja, E.; Álvarez-Valdés, A.; Pérez, J. M.; Navarro-Ranninger, C.; Reedijk, J.; *Inorg. Chim. Acta*, **2002**, 339, 525

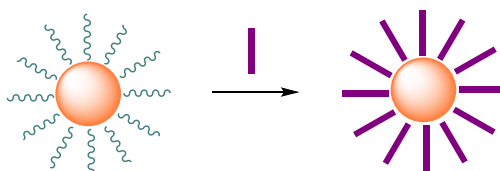
## 5. Surface Functionalization of Colloidal Nanocrystals

The ligand molecules that coat the surface of colloidal NCs, forming the surfactant (or capping) layer, have a strong influence in the nucleation and growth kinetics, thereby controlling their size and shape. In addition, several physico-chemical properties are directly determined by the organic surfactant layer and by the organic–inorganic interface, and can thus be manipulated by an adequate choice of ligands. Typically, NCs surfactants consist of a non-polar tail (which determines the interaction of the surfactant layer with the surrounding medium) and a polar head group whose ability to bind to the NC surface comes from the presence of donor atoms (N, O, S, P) with unshared electron pairs capable of forming coordinating bonds with metal atoms or ions.<sup>[33]</sup>

Colloidal NCs are commonly synthesized with a hydrophobic surfactant layer, making them readily dispersible in non-polar solvents. However, some applications, like biomedical imaging, require water-dispersible NCs, which can be achieved by simply exchanging the native hydrophobic ligands by hydrophilic or charged ones.

The most widely used procedure for surface functionalization of colloidal NCs involves the displacement of the native surfactant (Scheme 9) with difunctional molecules containing a surface-binding head group at one end and the desired functional group at the other end. The native surfactant molecules can easily be exchanged by stronger ligands, but in order to exchange the native ligand by a weaker one (i.e. fatty acids by amines) or by one with a comparable binding strength, it is necessary to use a large excess of the new ligand.<sup>[34]</sup>

Several techniques can be used to study the ligand exchange process. Since the Photoluminescence (PL) of colloidal semiconductor NCs is influenced by the nature of the surfactant layer, commonly used optical spectroscopy techniques can provide information about surface modification. In fact, surface reactions can affect the PL of colloidal NCs so dramatically that it could lead to PL enhancement or quenching,<sup>[35]</sup> depending on the chemical nature of the new surfactant and the extent of the exchange.



Scheme 9.- Ligand exchange

<sup>33</sup> De Mello Donegá, C.; *Chem. Soc. Rev.*, **2011**, *40*, 1512

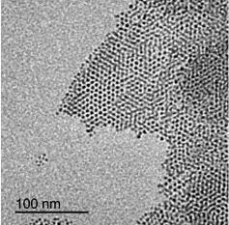
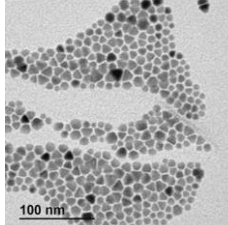
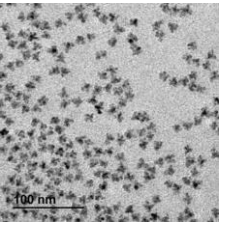
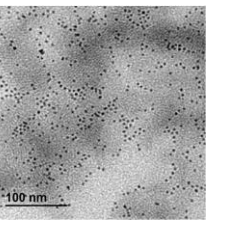
<sup>34</sup> Wuister, S. F.; Van Houselt, A.; De Mello Donegá, C.; Vanmaekelbergh, D.; Meijerink, A.; *Angew. Chem., Int. Ed.*, **2004**, *43*, 3029

<sup>35</sup> Bullen, C.; Mulvaney, P.; *Langmuir*, **2006**, *22*, 3007.

## 5.1. Synthesis and characterization of colloidal nanocrystals

Although the synthesis and characterization of colloidal NCs was not part of this work, the knowledge of the NCs characteristics was essential to control the ligand exchange process. In this work, four different NCs were selected (Table 4) to study the affinity between the amine ending group of our ligands and the inorganic NC surface:

- The synthesis of Ag<sub>2</sub>S NCs was performed by thermal decomposition of silver diethyldithiocarbamate with 1-dodecanethiol (DDT).<sup>[36]</sup>
- Colloidal semiconductor CdSe NCs were prepared by hot injection method. When reacting CdO (cadmium precursor) and octadecylphosphonic acid (ODPA), using trioctylphosphine oxide (TOPO) as reaction medium, the Cd-ODPA complex was formed. In a second step, Se dissolved in trioctylphosphine (TOP) was injected at high temperature and, finally, Cl<sup>-</sup> ions were added to the ligand shell by addition of dichloroethane (DCE).<sup>[37]</sup>
- Alloyed semiconductor CdSe/ZnS NCs were synthesized using CdO, zinc stearate and oleic acid (OA). Once Cd(OA)<sub>2</sub> and Zn(OA)<sub>2</sub> were formed, a solution of Se and S in TOP was added. The NCs were grown for 2-10 min and DDT was finally added to the solution.<sup>[38]</sup>
- Core-Shell semiconductor CdSe/ZnS NCs were prepared by adding a solution of Se in 1-octadecene (ODE) to a mixture of CdO, OA and ODE. After the CdSe NCs formation, zinc diethyldithiocarbamate was used as precursor for ZnS shell growth.<sup>[39]</sup>

Sample Name	P2-15	L64	M133	M136
TEM Image				
Nanocrystal Composition	Ag <sub>2</sub> S	CdSe	CdSeZnS	CdSe/ZnS
Ligands Shell	DDT	Cl <sup>-</sup> , ODPA	DDT, OA	Oleylamine
Fluorescence Region	IR	UV	UV	UV

**Table 4.-** Properties and composition of the selected NCs

<sup>36</sup> Zhang, Y.; Hong, G.; Zhang, Y.; Chen, G.; Li, F.; Dai, H.; Wang, Q.; *ACS Nano*, **2012**, *6*, 3695

<sup>37</sup> Palencia, C.; Lauwaet, K.; De la Cueva, L.; Acebrón, M.; Conde, J. J.; Meyns, M.; Klinke, C.; Gallego, J. M.; Otero, R.; Hernández, B.; *Nanoscale*, **2014**, *6*, 6812

<sup>38</sup> Acebrón, M.; Galisteo-López, J. F.; Granados, D.; López-Ogalla, J.; Gallego, J. M.; Otero, R.; López, C.; Hernández, B.; *ACS Appl. Mater. Interfaces*, **2015**, *7*, 6935

<sup>39</sup> Dai, M. Q.; Lanry Yung, L. Y. L.; *Chem. Mater.* **2013**, *25*, 2193

## 5.2. Ligand exchange process

### 5.2.1. Ligand removal

In order to provide new properties or functionality to the given NCs, the ligand molecules of the surface can be modified. In organic solvents, these ligands undergo dynamic binding and unbinding processes that could lead to the ligand loss. This process can be eased by an excessive washing of the nanoparticles, facilitating the subsequent incorporation of new ligands to the surface. The ligand removal generates defects on the surface, giving rise to localized surface states which can act as non-radiative pathways and decrease the PL. This behaviour can be observed by monitoring the PL after successive washings cycles (consisting of sonication, centrifugation, decantation and resuspension in organic solvent), noticing a decrease in the PL over the number of washing cycles (Figure 11).

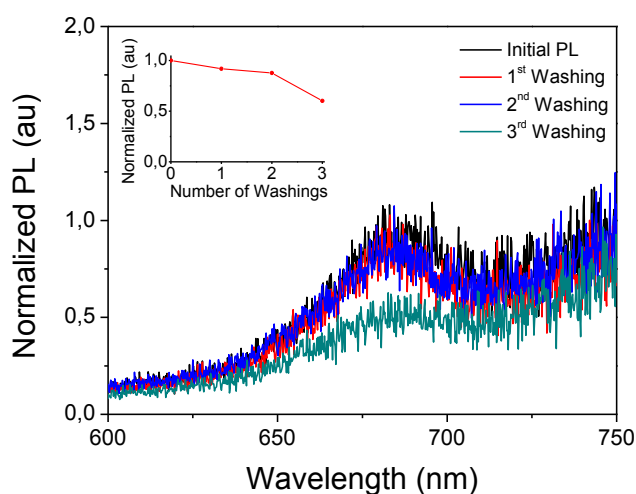


Figure 11.- Follow-up work for L64 NCs after several washings

### 5.2.2. Affinity study

Since we were trying to replace stronger ligands by weaker ones, a large excess of the new ligand was required. The CdSe concentration ( $[CdSe]$ ) in the samples was estimated according to some studies in which modifications to the Beer-Lambert led in a concentration dependence of the NCs optical absorption coefficient at both the band-edge and high within the absorption profile.<sup>[40]</sup> Known the  $[CdSe]$ , a molar ratio of Ligand:QD  $\approx 10^3:1$  was established to promote the ligand exchange.<sup>[39]</sup>

To determine the reaction parameters, all four types of NCs were incubated with commercially available 1,3-bis(3-aminopropyl)-1,1,3,3-tetramethyldisiloxane as replacing ligand, at room temperature and under vigorous stirring for 6 days. Afterwards, the samples were washed several times, in cycles of centrifugation and sonication, to eliminate the ligand excess.

<sup>40</sup> Jasieniak, J.; Smith, L.; Van Embden, J.; Mulvaney, P.; *J. Phys. Chem. C*, **2009**, *113*, 19468

Ag<sub>2</sub>S incubated NCs were studied by FT-IR (Fourier Transform Infrared Spectroscopy). No difference was found between the final IR spectra and the **P2-15** initial one, proving that there was not a ligand exchange process. This was probably related to the lower affinity of the amine groups to the silver atoms present at the NCs surface, compared to the original organic shell (DDT), whose thiolated ligands were strongly bonded to the surface and made difficult the ligand substitution.

On the other hand, better results were obtained with CdSe NCs. The PL signal was monitored over the hours, showing good results for both **L64** and **M136**, which evidenced an improvement in their optical properties. In the case of **L64**, PL enhancement was observed after a 24 h treatment (Figure 12a) but a 48 h treatment was necessary for the **M136** sample (Figure 12b). PL quenching was observed for longer reaction times, probably related to the NCs aggregation, a feasible phenomenon since the amine group at each terminal of the ligand probably leads to the formation of dimmers bridged by the ligand. In addition, **M136** presented a slight PL peak blue-shift as a consequence of the reduction in the effective size of CdSe by ligand exchange.<sup>[41]</sup>

On the contrary, the PL quenching (Figure 12c) of **M133** could be explained by an electronic coupling between NCs, consistent with the red-shifted PL spectra.

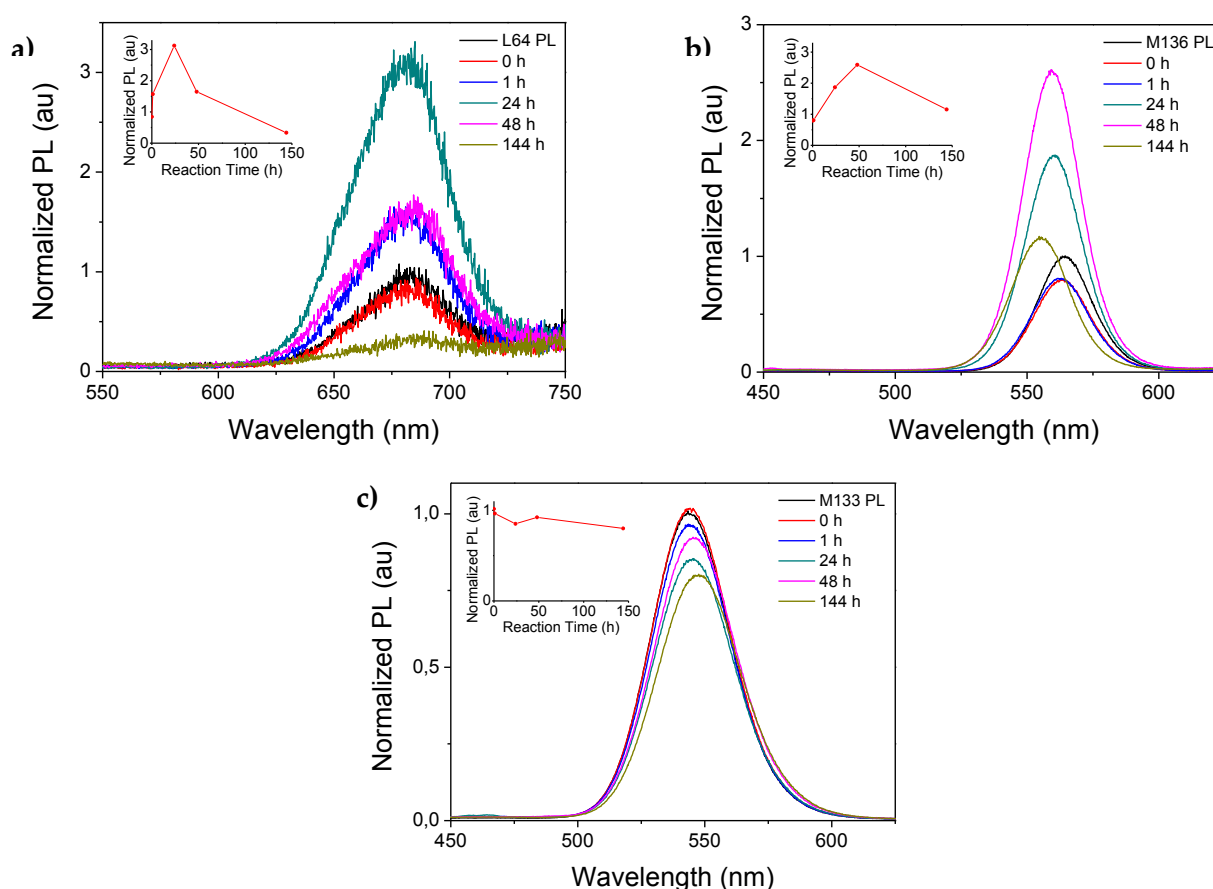


**Figure 12.-** PL signal follow-up work for **a) L64**, **b) M136** and **c) M133** CdSe NCs. All PL curves have been normalized taking the initial NC PL as relative value.

<sup>41</sup> Luo, X.; Liu, P.; Truong, N. T. N.; Farva, U.; Park, C.; *J. Phys. Chem.*, **2011**, *115*, 20817

Other techniques were used to complete the NCs characterization. Transmission Electron Microscopy (TEM) images were in agreement with the observed optical properties since, for instance, NCs aggregation was evident for **M133** NCs (Figure 13b). Meanwhile, **L64** NCs were much less aggregated and it was even possible to appreciate a capping shell around the inorganic NCs (Figure 13a). However, further FT-IR characterization of **L64** brought unexpected results. Although signals in the 800 - 1200  $\text{cm}^{-1}$  region were clearly attributed to Si-O-Si bond vibrations, the absence of the N-H stretching vibration signal at 3300 - 3400  $\text{cm}^{-1}$  suggested a possible degradation of the polymer, leading to the formation of a  $\text{SiO}_2$  coverage.

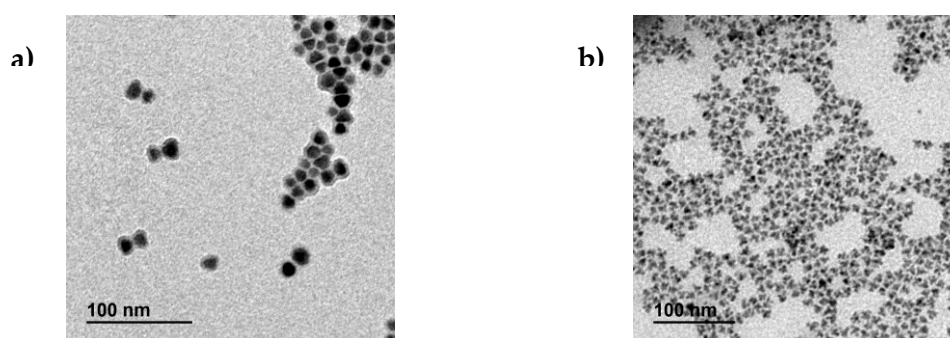


Figure 13.- TEM images of a) **L64** and b) **M133** CdSe NCs.

Regarding incubated **M136** NCs, FT-IR provided evidence of a successful ligand exchange process. In Figure 14, the dashed rectangles indicate the presence of both N-H and Si-O-Si bond vibrations in comparison with the original **M136** NCs and the replacing ligand FT-IR spectra.

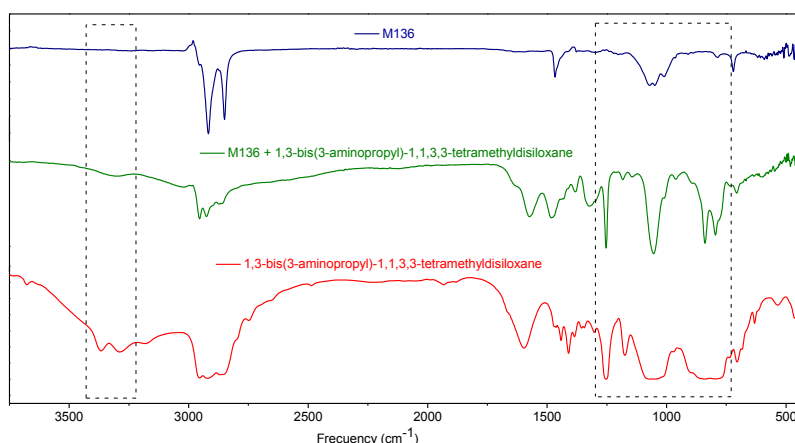


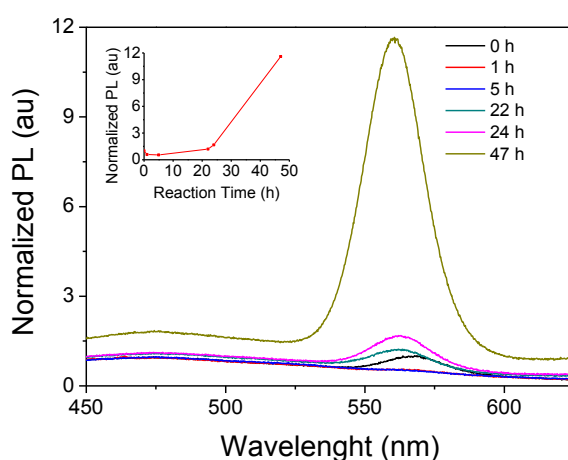
Figure 14.- FT-IR spectra of the original **M136** NCs (blue), the replacing ligand (red) and the incubated NCs

### 5.2.3. Ligand exchange

Considering this study, just **M136** showed sufficiently positive results to undergo the ligand exchange process. Although the objective was to incubate **M136** NCs with dendrimer-platinum(II) conjugate (**7**), N-BOC protected siloxane (**3**) was finally chosen as replacing ligand.

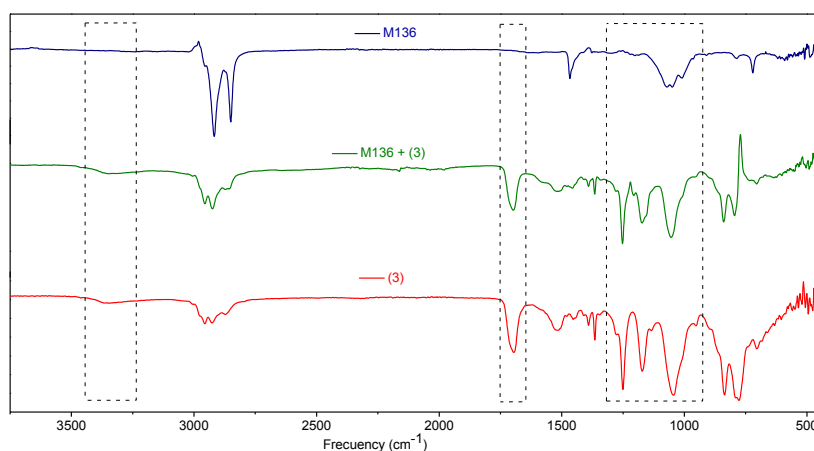
As mentioned before, **M136** NCs were successively washed to remove the original organic ligands and ease the incorporation of **(3)** to the surface. Afterwards, **M136** NCs were incubated with **(3)** at room temperature under vigorous stirring for 48 h. Finally, the sample was washed several times, to eliminate the ligand excess.

Figure 15 shows the evolution of the incubated NCs PL obtained at different reaction times, noticing a remarkable improvement in the NCs optical properties. This PL enhancement was related to the ligand exchange process, probably due to the nature of the ligand, which provides proper capping of the surface traps favouring radiative recombinations. In addition, the N-BOC protected part prevented the formation of aggregates, avoiding the corresponding PL quenching.



**Figure 15.-** PL signal follow-up work for **M136** NCs. All PL curves have been normalized taking the initial NC PL as relative value.

Besides, FT-IR characterization agreed with the observed optical properties. Figure 16 show the appearance of the N-H ( $3300 - 3400 \text{ cm}^{-1}$ ), the C=O ( $\sim 1700 \text{ cm}^{-1}$ ) and the Si-O-Si vibration bands ( $800 - 1200 \text{ cm}^{-1}$ ).



**Figure 16.-** FT-IR spectra of the original **M136** NCs (blue), the replacing ligand **(3)** (red) and the incubated NCs (green).

## 6. Experimental

All reactions and compound manipulations were performed under an inert atmosphere using standard Schlenk techniques. Solvents were dried with proper drying agents, according to the methods described in the bibliography,<sup>[42]</sup> and were distilled immediately prior to use.

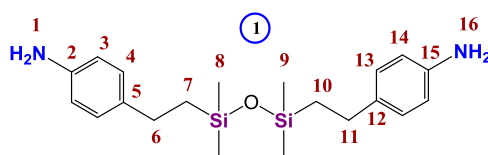
Infrared spectra were recorded on Perkin-Elmer 100 FT-IR spectrometer, between 4000 y 250  $\text{cm}^{-1}$ , using ATR (Attenuated Total Reflection) for solid compounds and CsI windows for oily compounds. Both  $^1\text{H-NMR}$  and  $^{13}\text{C-NMR}$  were recorded on Bruker-AMX-300 and on Bruker DRX-500 spectrometers. In addition,  $^{195}\text{Pt-NMR}$  spectra were done at SIdI (Servicio Interdepartamental de Investigación) on a Bruker Avance III-HD Nanobay 300MHz, while Mass analysis was made on Bruker Analyser ULTRAFLEX III (MALDI-TOF/TOF), ABSciex QSTAR (ESI) and Water VG AutoSpec (FAB).

Optical absorption measurements were carried out using a Varian Spectrophotometer Cary 50. Photoluminescence spectra were recorded in a spectrofluorometer Horiba Jobin Yvon Fluoromax-4. TEM (Transmission Electron Microscopy) images were obtained in a JEOL 1010 Microscope, operating with an acceleration voltage of 100 kV.

### 6.1. Synthesis of $\{(\text{CH}_3)_2\text{Si}[p\text{-(CH}_2)_2\text{C}_6\text{H}_4\text{NH}_2]\}_2\text{O}$ (**1**) (Scheme 2)

To a solution of commercially available 1,1,3,3-tetramethyldisiloxane (1.0 mL, 5.6 mmol) in dry toluene (10.0 mL) at 45°, 4-vinylaniline (1.3 g, 11.0 mmol) and *Karstedt Catalyst* (350  $\mu\text{L}$ ) were added. The reaction mixture was refluxed and stirred under argon atmosphere. After 72 h, the solvent was removed under reduced pressure and the residue was chromatographed on a silica gel column using dichloromethane/acetone (10:1) to give (**1**) as a yellow oil.

**Yield:** 0.77 g (36%).  $^1\text{H-NMR}$  ( $\text{CDCl}_3$ , 300 MHz):  $\delta$  0.11 (s, 12H, H8/H9), 0.89 (m, 4H, H7/H10), 2.58 (m, 4H, H6/H11), 3.55 (br, 4H, H1/H16), 6.62 (d, AA' part of AA'BB'  $^3\text{J} = 6$  Hz, 2H, H3/H14), 7.00 (d, BB' part of AA'BB'  $^3\text{J} = 6$  Hz, 2H, H4/H13).  $^{13}\text{C-NMR}$  ( $\text{CDCl}_3$ , 300 MHz):  $\delta$  0.32 (C8/C9), 20.4 (C7/C10), 28.5 (C6/C11), 115.5 (C3/C14), 128.7 (C4/C13), 135.2 (C5/C12), 144.0 (C2/C15). **FTIR** (CsI,  $\text{cm}^{-1}$ ):  $\nu(\text{NH}_2)$  3350, 3223;  $\nu(\text{C-H})$  2957;  $\delta(\text{NH}_2)$  1623;  $\nu(\text{Ar})$  1515;  $\nu(\text{Si-CH}_3)$  1256;  $\nu(\text{Si-O-Si})$  1060;  $\delta(\text{Si-CH}_3)$  840, 795. **MS (FAB<sup>+</sup>):** m/z 372 [ $\text{M}^+$ ].



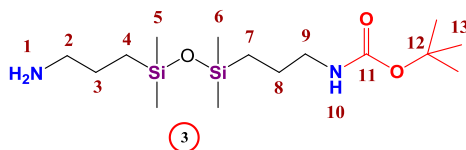
<sup>42</sup> Perrin, D. D.; Armarego, W. L. F. *Purification of Laboratory Chemicals*; Pergamon Press Ltd. 2<sup>nd</sup> ed. Oxford, 1980

## 6.2. Synthesis of N-BOC protected siloxanes (3) and (4) and ferrocene-containing siloxane (5)

### 6.2.1. Preparation of {BOCNH(CH<sub>2</sub>)<sub>3</sub>Si(CH<sub>3</sub>)<sub>2</sub>}O{(CH<sub>3</sub>)<sub>2</sub>Si(CH<sub>2</sub>)<sub>3</sub>NH<sub>2</sub>} (3) (Scheme 4)

1,3-bis(3-aminopropyl)-1,1,3,3-tetramethyldisiloxane (2.2 mL, 8.0 mmol) was dissolved in ethanol (3.0 mL). The stirred solution was externally cooled with an ice bath and (BOC)<sub>2</sub>O (0.22 g, 1.0 mmol) in ethanol (3.0 mL) was slowly added, over a period of 2.5 h. The reaction was allowed to proceed at room temperature for another 22 h under argon atmosphere. The solvent was removed and the crude product was purified by column chromatography on silica gel using *n*-hexane/EtOH (3:1) as eluent, giving (3) as a yellow oil.

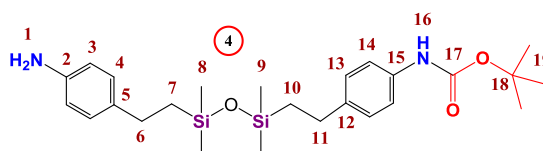
**Yield:** 0.26 g (75%). <sup>1</sup>H-NMR (CDCl<sub>3</sub>, 300 MHz): δ 0.04 (s, 12H, H<sub>5</sub>/H<sub>6</sub>), 0.49 (m, 4H, H<sub>4</sub>/H<sub>7</sub>), 1.41 (br, 2H, H<sub>8</sub>) 1.42 (br, 2H, H<sub>3</sub>), 1.43 (s, 9H, H<sub>13</sub>), 1.74 (br s, 2H, H<sub>1</sub>), 2.73 (t, <sup>3</sup>J = 6 Hz, 2H, H<sub>2</sub>), 3.08 (q, <sup>3</sup>J = 6 Hz, 2H, H<sub>9</sub>), 4.70 (br s, 1H, H<sub>10</sub>). <sup>13</sup>C{<sup>1</sup>H}-NMR (CDCl<sub>3</sub>, 300 MHz): δ 0.32 (C<sub>5</sub>/C<sub>6</sub>), 15.40 (C<sub>4</sub>/C<sub>7</sub>), 24.02 (C<sub>3</sub>/C<sub>8</sub>), 28.45 (C<sub>13</sub>), 43.52 (C<sub>9</sub>), 45.18 (C<sub>2</sub>), 78.83 (C<sub>12</sub>), 156.02 (C<sub>11</sub>). IR (CsI, cm<sup>-1</sup>): ν(N-H) 3350; ν(C-H) 2956, 2927; ν(C=O) 1695; ν(Si-CH<sub>3</sub>) 1251; ν(C-N) 1172; ν(Si-O-Si) 1043; δ(Si-CH<sub>3</sub>) 836, 777. MS (MALDI): m/z 349.3 [M+H]<sup>+</sup>.



### 6.2.2. Preparation of {BOCNH[p-C<sub>6</sub>H<sub>4</sub>(CH<sub>2</sub>)<sub>2</sub>]Si(CH<sub>3</sub>)<sub>2</sub>}O{(CH<sub>3</sub>)<sub>2</sub>Si[p-(CH<sub>2</sub>)<sub>2</sub>C<sub>6</sub>H<sub>4</sub>NH<sub>2</sub>]} (4) (Scheme 5)

To an externally cooled solution of (1) (0.42 g, 1.1 mmol) in ethanol (1.0 mL), another solution of (BOC)<sub>2</sub>O (60 mg, 0.28 mmol) in ethanol (0.8 mL) was slowly added over a period of 8 h. The reaction was allowed to proceed at room temperature for another 22 h under argon atmosphere. The solvent was removed and the crude product was purified by column chromatography on silica gel using *n*-hexane/EtOH (8:1) as eluent, giving (4) as a yellow oil.

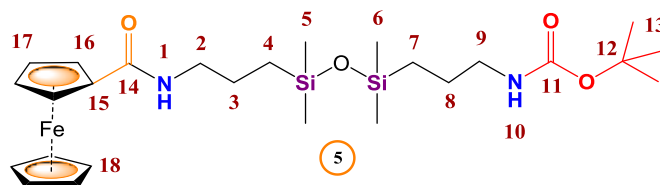
**Yield:** 96 mg (74%). <sup>1</sup>H-NMR (CDCl<sub>3</sub>, 300 MHz): δ 0.12 (s, 12H, H<sub>8</sub>/H<sub>9</sub>), 0.89 (m, 4H, H<sub>7</sub>/H<sub>10</sub>), 1.51 (br, 9H, H<sub>19</sub>), 2.59 (m, 4H, H<sub>6</sub>/H<sub>11</sub>), 3.52 (br, 2H, H<sub>1</sub>), 6.38 (br, 1H, H<sub>16</sub>), 6.62 (d, AA' part of AA'BB' <sup>3</sup>J = 6 Hz, 2H, H<sub>3</sub>), 7.00 (d, BB' part of AA'BB' <sup>3</sup>J = 6 Hz, 2H, H<sub>4</sub>), 7.12 (d, AA' part of AA'BB' <sup>3</sup>J = 6 Hz, 2H, H<sub>13</sub>), 7.25 (d, BB' part of AA'BB' <sup>3</sup>J = 6 Hz, 2H, H<sub>14</sub>). <sup>13</sup>C-NMR (CDCl<sub>3</sub>, 300 MHz): δ 0.30 (C<sub>8</sub>/C<sub>9</sub>), 20.4 (C<sub>7</sub>/C<sub>10</sub>), 28.3 (C<sub>19</sub>), 28.5 (C<sub>6</sub>), 28.6 (C<sub>11</sub>), 80.1 (C<sub>18</sub>), 115.3 (C<sub>3</sub>), 118.7 (C<sub>14</sub>), 128.1 (C<sub>13</sub>), 128.4 (C<sub>4</sub>), 135.2 (C<sub>5</sub>), 135.8 (C<sub>15</sub>), 139.8 (C<sub>12</sub>), 143.8 (C<sub>2</sub>), 152.9 (C<sub>17</sub>). IR (ATR, cm<sup>-1</sup>): ν(N-H) 3334; ν(C-H) 2958; ν(C=O) 1702; ν(Ar) 1516; ν(Si-CH<sub>3</sub>) 1252; ν(C-N) 1159; ν(Si-O-Si) 1048; δ(Si-CH<sub>3</sub>) 834, 780. MS (MALDI): m/z 473.3 [M+H]<sup>+</sup>.



### 6.2.3. Preparation of {BOCNH(CH<sub>2</sub>)<sub>3</sub>Si(CH<sub>3</sub>)<sub>2</sub>}O{(CH<sub>3</sub>)<sub>2</sub>Si(CH<sub>2</sub>)<sub>3</sub>NHCOFc} (5) (Scheme 6)

Ferrocenecarboxylic acid (34 mg, 0.15 mmol), HOBT (20 mg, 0.15 mmol) and EDC (26  $\mu$ L, 0.15 mmol) were dissolved in 25.0 mL of cooled dry CH<sub>2</sub>Cl<sub>2</sub> and the resulting mixture was stirred and treated with (3) (105 mg, 0.30 mmol). After the addition, stirring was continued for 30 min at 0° C and then at room temperature overnight. The mixture was extracted with water, dried over MgSO<sub>4</sub>, and evaporated under vacuum to give (5) as an orange oil.

**Yield:** 28 mg, (33%). <sup>1</sup>H-NMR (CDCl<sub>3</sub>, 300 MHz):  $\delta$  0.07 (s, 12H, H<sub>5</sub>/H<sub>6</sub>), 0.53 (m, 4H, H<sub>4</sub>/H<sub>7</sub>), 1.45 (s, 9H, H<sub>13</sub>), 1.60 (br, 4H, H<sub>3</sub>/H<sub>8</sub>), 3.11 (br, 2H, H<sub>9</sub>), 3.36 (b, 2H, H<sub>2</sub>), 4.20 (s, 5H, H<sub>18</sub>), 4.33 (br, 2H, H<sub>17</sub>), 4.70 (br, 2H, H<sub>16</sub>), 4.82 (br, 1H, H<sub>10</sub>), 5.95 (br, 1H, H<sub>1</sub>). <sup>13</sup>C{<sup>1</sup>H}-NMR (CDCl<sub>3</sub>, 300 MHz):  $\delta$  0.51 (C<sub>5</sub>/C<sub>6</sub>), 15.60 (C<sub>7</sub>), 15.8 (C<sub>4</sub>) 24.1 (C<sub>8</sub>), 24.2 (C<sub>3</sub>) 28.63 (C<sub>13</sub>), 42.6 (C<sub>9</sub>), 45.18 (C<sub>2</sub>), 68.2 (C<sub>16</sub>), 69.9 (C<sub>18</sub>), 70.4 (C<sub>17</sub>), 76.7 (C<sub>15</sub>), 79.1 (C<sub>12</sub>), 156.2 (C<sub>11</sub>), 170.1 (C<sub>14</sub>). IR (CsI, cm<sup>-1</sup>):  $\nu$ (N-H) 3327;  $\nu$ (C-H) 2949 2920;  $\nu$ (C=O) 1695, 1638;  $\nu$ (Si-CH<sub>3</sub>) 1248;  $\nu$ (C-N) 1175;  $\nu$ (Si-O-Si) 1055;  $\delta$ (Si-CH<sub>3</sub>) 843, 785. MS (ESI): m/z 561.3 [M+H]<sup>+</sup>.



## 6.3. Synthesis of *cis*-[PtCl<sub>2</sub>(DMSO)<sub>2</sub>] complex (6) and dendrimer-platinum(II) conjugate (7)

### 6.3.1. Preparation of *cis*-[PtCl<sub>2</sub>(DMSO)<sub>2</sub>] (6) (Scheme 7)

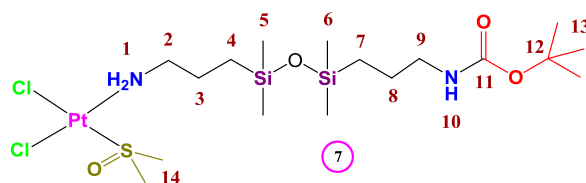
According to the method described in the literature,<sup>[6]</sup> DMSO (1.1 mL, 15.0 mmol) was added to a solution of K<sub>2</sub>[PtCl<sub>4</sub>] (2.1 g, 5.0 mmol) in distilled water (21.0 mL). The mixture was stirred at room temperature for 24 h and the isolated yellow solid was separated by filtration, washed with water, ethanol and diethyl ether, and dried under vacuum.

**Yield:** 1.72 g (80%).

### 6.3.2. Preparation of *cis*-[PtCl<sub>2</sub>(DMSO)([NH<sub>2</sub>(CH<sub>2</sub>)<sub>3</sub>O]Si{O(CH<sub>2</sub>)<sub>3</sub>NHBOC})] (7) (Scheme 8)

A solution of (3) (0.10 g, 0.3 mmol) in 1.0 mL of CH<sub>2</sub>Cl<sub>2</sub> was added to a solution of *cis*-[PtCl<sub>2</sub>(DMSO)<sub>2</sub>] (6) (0.12 g, 0.30 mmol) in 4.0 mL of the same solvent. The mixture was stirred at room temperature for 24 h and the resulting solution was concentrated under vacuum to give an orange oil. The addition of diethyl ether led to a white solid precipitation, which was filtered off. The remaining orange oil was washed with diethyl ether and dried under vacuum to give (7) as an orange oil.

**Yield:** 185 mg (90%). **<sup>1</sup>H-NMR (CDCl<sub>3</sub>, 300 MHz):** δ 0.05 (s, 12H, H5/H6), 0.50 (m, 4H, H4/H7), 1.43 (br, 2H, H8), 1.43 (s, 9H, H13), 1.65 (br s, 2H, H3), 2.87 (m, 2H, H2), 3.07 (m, 2H, H9), 3.38 (s, 6H, H14), 4.14 (br, 2H, H1), 4.66 (br, 1H, H10). **<sup>13</sup>C{<sup>1</sup>H}-NMR (CDCl<sub>3</sub>, 300 MHz):** δ 0.41 (C5/C6), 15.07 (C4), 15.42 (C7), 24.07 (C8), 25.10 (C3) 28.49 (C13), 41.04 (C14), 43.75 (C9), 48.75 (C2), 79.0 (C12), 156.04 (C11). **IR (CsI, cm<sup>-1</sup>):** ν(N-H) 3581; ν(C-H) 2959, 2919; ν(C=O) 1707; ν(Si-CH<sub>3</sub>) 1255; ν(C-N) 1179; ν(Si-O-Si) 1049; δ(Si-CH<sub>3</sub>) 844, 785. **MS (ESI):** m/z 693 [M+H]<sup>+</sup>.



#### 6.4. General procedure for ligand exchange incubation

QDs in 0.25 mL of stock solution, redispersed in 1.0 mL of chloroform, were successively washed by ethanol-induced flocculation and centrifugation. After an excessive washing, the supernatant was decanted and the pellet was redispersed in 2.0 mL of chloroform and loaded in a UV/VIS Cell. The proper portion of ligand (Table 5) was added to the solution under vigorous stirring. Because of the high solubility of the ligands in chloroform, no phase separation was observed. After the corresponding reaction time, ethanol in excess was added to the solution and the QDs were precipitated out of the crude solution by centrifugation.

Sample Name	Affinity study				Ligand Exchange			
	P2-15	L64	M133	M136	L64	M136	L64	M136
Nanocrystal Composition	Ag <sub>2</sub> S	CdSe	CdSeZnS	CdSe/ZnS	CdSe	CdSe/ZnS	CdSe	CdSe/ZnS
Estimated Concentration (M)	~ 10 <sup>-6</sup>	~ 10 <sup>-7</sup>	~ 10 <sup>-7</sup>	~ 10 <sup>-7</sup>	~ 0.5 · 10 <sup>-6</sup>	~ 10 <sup>-6</sup>	~ 0.5 · 10 <sup>-6</sup>	~ 10 <sup>-6</sup>
Replacing Ligand	1,3-bis(3-aminopropyl)-1,1,3,3-tetramethyldisiloxane						(3)	(3)
Amount of Ligand	250 μL	30 μL	30 μL	30 μL	150 μL	165 mg	200 mg	280 mg

**Table 5.-** Concentration values for the ligand exchange reactions

## 7. Conclusions and Future Work

---

Application of dendritic molecules, platinum(II) complexes, ferrocene and colloidal NCs in cancer therapeutics are active research areas that we have tried to connect in this work. Thus, four siloxane derivatives and one dendrimer-platinum(II) conjugate were successfully designed, synthesized and characterized, allowing us to conclude that:

- ✿ Hydrosilylation of olefins turned to be adequate to synthesize homofunctionalized siloxanes such as  $\{(\text{CH}_3)_2\text{Si}[p\text{-(CH}_2)_2\text{C}_6\text{H}_4\text{NH}_2]\}_2\text{O}$  (**1**), but resulted ineffective when trying to synthesize heterofunctionalized siloxanes, like  $\{[p\text{-NH}_2\text{C}_6\text{H}_4(\text{CH}_2)_2]\text{Si}(\text{CH}_3)_2\}_2\text{O}\{(\text{CH}_3)_2\text{Si}[(\text{CH}_2)_2(\text{Fc})]\}$  (**2**).
- ✿ The synthesis of BOC protected siloxanes  $\{\text{BOCNH}(\text{CH}_2)_3\text{Si}(\text{CH}_3)_2\}_2\text{O}\{(\text{CH}_3)_2\text{Si}(\text{CH}_2)_3\text{NH}_2\}$  (**3**) and  $\{\text{BOCNH}[p\text{-C}_6\text{H}_4(\text{CH}_2)_2]\text{Si}(\text{CH}_3)_2\}_2\text{O}\{(\text{CH}_3)_2\text{Si}[p\text{-(CH}_2)_2\text{C}_6\text{H}_4\text{NH}_2]\}$  (**4**) proved that selective BOC protection was a very useful mean to monofunctionalize symmetrical diamines.
- ✿ Although selective hydrosilylation with vinylferrocene was attempted, ferrocene-amide formation emerged as a suitable method to synthesize novel ferrocenyl-derivative siloxanes like  $\text{BOCNH}(\text{CH}_2)_3\text{Si}(\text{CH}_3)_2\}_2\text{O}\{(\text{CH}_3)_2\text{Si}(\text{CH}_2)_3\text{NHCOFc}\}$  (**5**).
- ✿ The synthesis of *cis*- $[\text{PtCl}_2(\text{DMSO})\{(\text{NH}_2(\text{CH}_2)_3\text{Si}(\text{CH}_3)_2\}_2\text{O}\{(\text{CH}_3)_2\text{Si}(\text{CH}_2)_3\text{NHBOC}\})]$  (**7**) confirmed that the presence of silicon enhances the solubility of this type of compounds in organic solvents and it improved the results obtained in our previous researches (Figure 3).<sup>[6]</sup>
- ✿ Despite studying different NCs, the ligand exchange incubation of (**3**) with core-shell semiconductor CdSe/ZnS (**M136**) NCs evidenced a remarkable and promising improvement on its optical properties.

Finally, when analysing these results and conclusions, some of our future outlooks may be:

- ✿ Evaluate the potential cytotoxicity of the novel designed dendrimer-platinum(II) conjugates.
- ✿ Use higher branched dendritic structures as precursors, looking for multiple functionalization.
- ✿ Modify the linking groups to the NCs, using stronger ligands (e.g. thiols) to improve the process both kinetically and thermodynamically.
- ✿ Study different types of nanoparticles to provide other remarkable properties (e.g. superparamagnetic  $\text{Fe}_3\text{O}_4$  nanoparticles).